Hindawi Publishing Corporation
Advances in OptoElectronics
Volume 2011, Article ID 194508, 5 pages
doi:10.1155/2011/194508

Research Article

Dye-Sensitized Solar Cells Based on High Surface Area Nanocrystalline Zinc Oxide Spheres

Pavuluri Srinivasu,[1] Surya Prakash Singh,[2] Ashraful Islam,[3,4] and Liyuan Han[3]

[1] *International Center for Young Scientists, International Center for Materials Nanoarchitectonics, National Institute for Materials Science, 1-1 Namiki, Tsukuba, Ibaraki 305-0044, Japan*
[2] *Inorganic and Physical Chemistry Division, Indian Institute of Chemical Technology, Hyderabad 500007, India*
[3] *Advanced Photovoltaics Center, National Institute for Materials Science, 1-2-1 Sengen, Tsukuba, Ibaraki 305-0047, Japan*
[4] *Center of Excellence for Research in Engineering Materials (CEREM), College of Engineering, King Saud University, Riyadh 11421, Saudi Arabia*

Correspondence should be addressed to Pavuluri Srinivasu, pavuluri.srini@gmail.com

Received 30 April 2011; Accepted 26 May 2011

Academic Editor: Idriss M. Bedja

High surface area nanocrystalline zinc oxide material is fabricated using mesoporous nanostructured carbon as a sacrificial template through combustion process. The resulting material is characterized by XRD, N_2 adsorption, HR-SEM, and HR-TEM. The nitrogen adsorption measurement indicates that the materials possess BET specific surface area ca. 30 m^2/g. Electron microscopy images prove that the zinc oxide spheres possess particle size in the range of 0.12 μm–0.17 μm. The nanocrystalline zinc oxide spheres show 1.0% of energy conversion efficiency for dye-sensitized solar cells.

1. Introduction

Dye-sensitized solar cells (DSCs) have attracted great attention, due its advantages such as low cost, easy fabrication, and high energy conversion efficiency over traditional Si-solar cells [1, 2]. DSCs are composed of porous nanostructured oxide film with adsorbed dye molecules as a dye-sensitized anode, an electrolyte containing iodide/triiodide redox couple, and a platinized fluorine-doped tin oxide (FTO) glass as the counter electrode [3–5]. In DSCs high-internal-surface-area and wide-band-gap semiconductor material with adsorbed dye as a photoanode plays an important role. The choice of semiconductor depends on its conduction band, density state that allows efficient electronic coupling with the dye energy level to facilitate charge separation and minimize recombination. Additionally, the semiconductor material must have high internal surface area to maximize light absorption by the dye monolayer with good electrical conductivity to the substrate. In general, anatase titania nanocrystals are used as recipient of injected electrons from optically excited dye and provide the conductive pathway to the circuit. To complete the cycle the redox species in electrolyte solution transport the hole from oxidized dye to counter electrode [6]. However, titania has low electron mobility and transport properties, which trigger electron recombination rate. Recently, zinc oxide materials have been paid great interest as an alternative for titania in DSCs as its energy band gap is similar to that of titania with higher electron mobility [7, 8]. Moreover, zinc oxide possesses tunable structural properties more than any other semiconductor materials. Recently, several researchers have been using mesoporous silica as a template to prepare different transition metal oxides [9–14]. But removal of silica from the composite is a relatively difficult task which requires either strong acid or strong base conditions.

Recent research work of Srinivasu et al. has demonstrated first example of highly efficient metal-free counter electrode for DSCs using large mesoporous carbon [15]. Here, we have demonstrated a novel method to prepare nanocrystalline zinc oxide using large porous carbon synthesized from ordered mesoporous silica (KIT-6), which has not been

studied yet as a hard template for the preparation of zinc oxide spheres in the open literature. In the present study, nanocrystalline zinc oxide spheres are fabricated using mesoporous carbon as a hard template through combustion technique. Thus obtained material is carefully characterized using various sophisticated techniques. Also, DSC performance of nanocrystalline zinc oxide spheres isinvestigated.

2. Experimental

2.1. Preparation of Mesoporous Carbon and Zinc Oxide Spheres. Ordered mesoporous carbon material referred to as LPC (large-porous carbon) is synthesized by pyrolysis of sucrose inside the large-pore mesoporous silica (KIT-6) synthesized at 100°C. In a typical synthesis of mesoporous carbon, 1 g of KIT-6 is added to a solution obtained by dissolving 0.75 g of sucrose and 5.0 g of water and keeping the mixture in an oven for 6 h at 100°C. Subsequently, the oven temperature was raised to 160°C for another 6 h. In order to obtain fully polymerized and carbonized sucrose inside the pores of silica template, 0.5 g of sucrose, 0.06 g of H_2SO_4, and 5.0 g of water are again added to the pretreated sample and the mixture is again subjected to the thermal treatment described above. Carbonization is performed at 900°C for 5 h under N_2 atmosphere. The resulting carbon/silica composite is treated with HF acid (5 wt%) at room temperature for the selective removal of silica. Zinc oxide spheres are prepared by adding 20 mL of zinc nitrate (1.5 mol L^{-1}) solution and stirring at room temperature for 6 h. The impregnated carbon material is dried at room temperature and heated under air at 550°C for 4 h. The final ZnO nanosphere material is used to prepare a film on FTO glass using doctor blade technique [16, 17], which is ultrasonically cleaned in ethanol prior to use.

Powder X-ray diffraction patterns were obtained through a Rigaku diffractometer using CuKα (λ = 0.154 nm) radiation. N_2 adsorption-desorption isotherms are measured at 77 K on a Quantachrome Autosorb 1 volumetric adsorption analyzer. Before the adsorption measurements, all samples are outgassed at 250°C in the port of the adsorption analyzer. The position of the maximum on pore size distribution is referred to as the pore diameter, which was calculated from adsorption branches by Barret-Joyner-Halenda (BJH) method. The HRTEM images are obtained with JEOL JEM-2100F. Hitachi S-4800 HR-FESEM is used to observe the morphology of the material.

2.2. Fabrication of Dye-Sensitized Solar Cell

2.2.1. Preparation of ZnO Electrode. The dye solutions (0.3 mM solution of N719 dye) were prepared in 1 : 1 acetonitrile and *tert*-butyl alcohol solvents. Deoxycholic acid as a coadsorbent was added to the dye solution at a concentration of 20 mM. The electrodes were immersed in the dye solutions and then kept at 25°C for 24 h to adsorb the dye onto the ZnO.

2.2.2. Preparation of Dye-Sensitized Solar Cell. Photovoltaic measurements were performed in a two-electrode sandwich cell configuration. The dye-deposited ZnO film and a platinum-coated conducting glass were used as the working electrode and the counter electrode, respectively. The two electrodes were separated by a surlyn spacer (40 μm thick) and sealed up by heating the polymer frame. The electrolyte was composed of 0.6 M dimethylpropyl-imidazolium iodide (DMPII), 0.05 M I_2, TBP 0.5 M, and 0.1 M LiI in acetonitrile (AN).

3. Results and Discussion

The powder X-ray diffraction (XRD) pattern for zinc oxide spheres is shown in Figure 1(a) with Bragg diffraction wide-angle reflections between 2θ = 10–70°, which are indexed as (100), (002), (101), (102), (110), (103), and (112) planes corresponding to the wurtzite-analogous structure of ZnO. It indicates that the material is pure zinc oxide as there are no other peaks found in the XRD pattern. The low-angle peak periodicity of the mesopore carbon is not observed in ZnO spheres, which is due to collapse of mesoporosity during the high-temperature treatment in presence of air. This also can be explained that the incomplete filling of mesoporous carbon by zinc precursor leading to the collapse of the porous structure during heat treatment. It is interesting to note that pure anatase titania has been prepared using mesoporous carbon template without any rutile and brookite phases by removing carbon template by simple combustion process. Figure 1(b) shows nitrogen adsorption-desorption isotherm measured at 77 K for ZnO spheres. The obtained BET specific surface area for ZnO sphere is 32 m^2/g.

The morphology of zinc oxide spheres is observed using HR-SEM (Figure 1(c)), which confirms that the morphology of mesoporous carbon was retained even after removal of carbon template. The prepared ZnO nanospheres possess particle size in the range of 0.12–0.17 μm. ZnO spheres are further confirmed by high-resolution transmission electron microscopy (Figure 1(d)). The selected area electron diffraction (SAED) pattern of ZnO spheres in Figure 1(e) shows diffuse rings which indicate the polycrystalline. The interplanar spacing (d) values obtained from XRD are summarized in the table, which are comparable with computed SAED pattern. It can be seen from Figure 1(e) that indexed SAED pattern is equivalent to the pattern of wurtzite ZnO. It is interesting to note that SAED pattern from HR-TEM matches well with data obtained from powder XRD. It is concluded that synthesized zinc oxide spheres from novel carbon templating technique are highly crystalline with wurtzite phase. IPCE spectra of ZnO spheres are shown in Figure 2(a).

Monochromatic incident photon-to-current conversion efficiency (IPCE) for the solar cell, plotted as a function of excitation wavelength, was recorded on a CEP-2000 system (Bunko-Keiki Co. Ltd.). IPCE at each incident wavelength was calculated from the equation given below, where I_{sc} is the photocurrent density at short circuit in mA cm^{-2} under monochromatic irradiation, q is the elementary charge, λ is the wavelength of incident radiation in nm, and P_0 is the incident radiative flux in Wm^{-2}

$$\mathrm{IPCE}(\lambda) = 1240\left(\frac{I_{\mathrm{SC}}}{q\lambda P_0}\right). \quad (1)$$

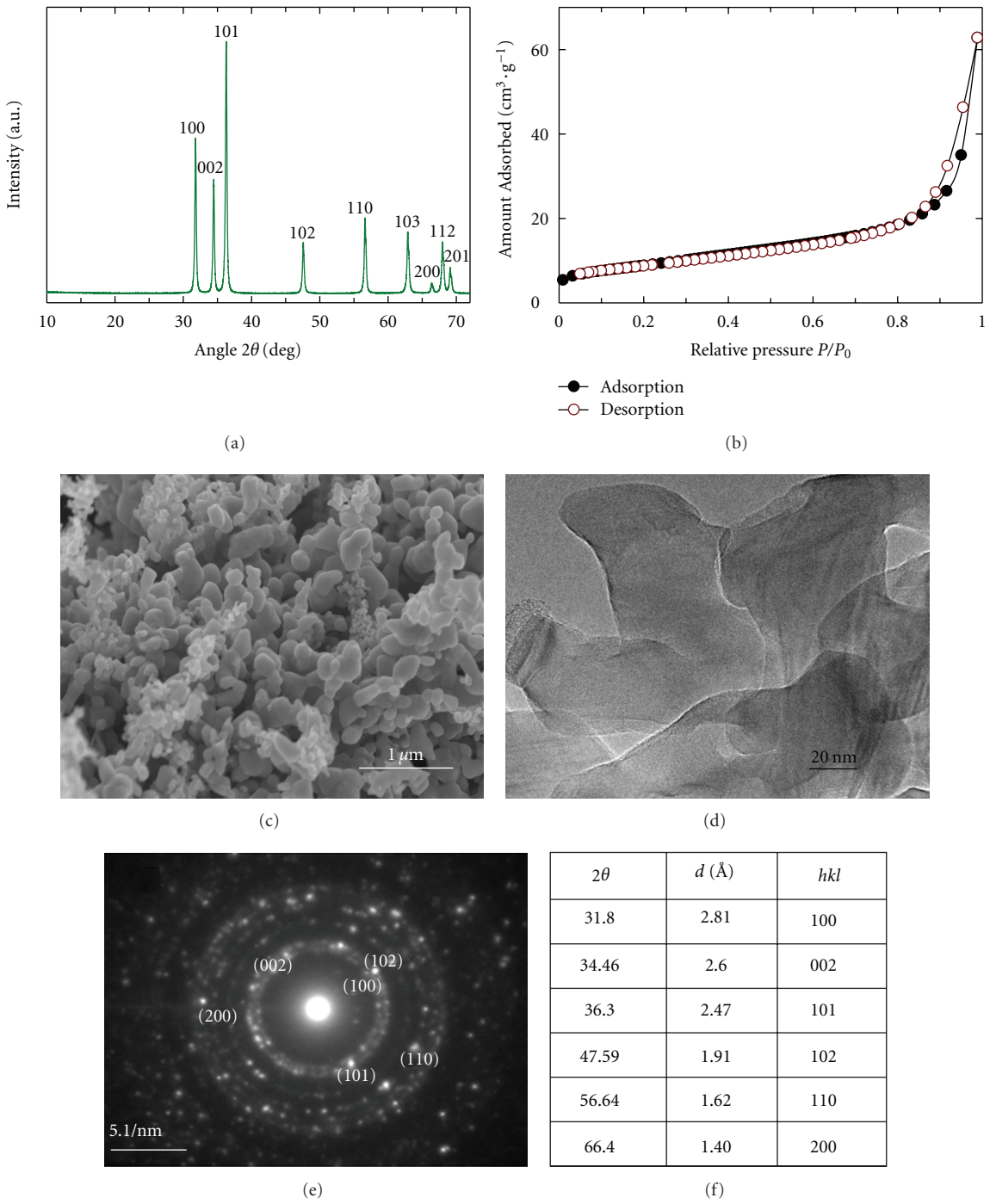

2θ	d (Å)	hkl
31.8	2.81	100
34.46	2.6	002
36.3	2.47	101
47.59	1.91	102
56.64	1.62	110
66.4	1.40	200

(f)

Figure 1: (a) X-ray diffraction pattern, (b) nitrogen adsorption isotherm of LPC material, (c) SEM image, (d) TEM image, and (e) selected area electron diffraction, (f) interplannar spacing values obtained from XRD of ZnO spheres.

The photocurrent density-voltage curves and incident photon-to-current efficiency (IPCE) spectra of the cells based on N719 dye under the illumination of air mass (AM) 1.5 sunlight (100 mW/cm^2, WXS-155S-10: Wacom Denso Co. Japan).

Usually the IPCE spectra at wavelength 500–600 nm are attributed to higher dye loading capacity of the material. Further the broad spectra between 600 and 750 nm a higher-wavelength region indicates that the N719 dye has low level of absorption for incident light and IPCE values higher than 600 nm can be ascribed to the enhanced light-scattering capacity of the material [18]. ZnO nanospheres show broad IPCE spectra between 500 and 600 nm indicating higher N719 dye absorption capacity. The materials also show little extended spectra in 600–700 nm region responsible for low level of dye absorption. The N719 dye on ZnO nanospheres

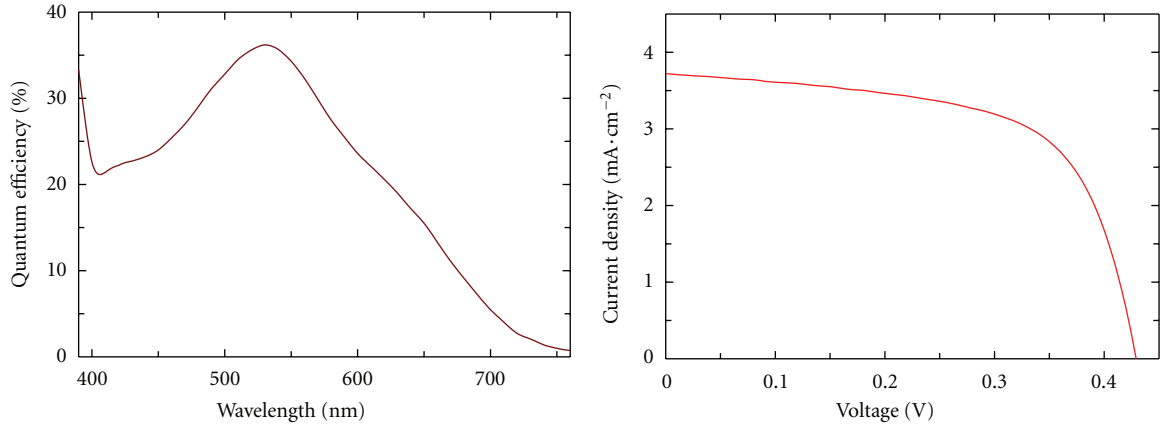

FIGURE 2: (a) Incident photon-to-current conversion efficiency (IPCE) spectra, (b) photocurrent-voltage *(I-V)* characteristics of dye-sensitized solar cells of ZnO nanospheres.

has maximum absorption of 35% at 530 nm. In conclusion, the IPCE spectra proves that higher-absorption property for dye molecule with little weak interaction between photons and the dye molecules on the ZnO crystallites.

Figure 2(b) shows the photocurrent density-photovoltage performance for DSCs based on ZnO nanospheres. The obtained short-circuit current (J_{sc}), the open-circuit voltage (V_{oc}), and the fill factor and (FF) for ZnO nanospheres are 3.7 mA/cm^2, 0.43 V, and 0.62%, respectively. The overall conversion efficiency (η) of 1.0% is obtained for ZnO nanospheres.

4. Conclusions

We have demonstrated dye-sensitized solar cells using ZnO nanospheres photoelectrode prepared using nanoporous carbon as template. The high-temperature heating process of mesoporous carbon and zinc precursor composite resulted in pure wurtzite-analogous structure of ZnO. The prepared ZnO nanospheres possess high surface area with particle size in the range of 0.12–0.17 μm. The dye-sensitized solar cells using ZnO spheres show 0.62% of fill factor and 1.0% of energy conversion efficiency.

Acknowledgment

P. Srinivasu thanks the International Center for Young Scientists (ICYS) and International Center for Materials Nanoarchitectonics (MANA) at National Institute for Materials Science, Tsukuba, Japan for financial support.

References

[1] M. K. Nazeeruddin, A. Kay, I. Rodicio et al., "Conversion of light to electricity by cis-X_2 bis(2,2′-bipyridyl-4,4′-dicarboxylate)ruthenium(II) charge-transfer sensitizers (X = Cl^-, Br^-, I^-, CN^-, and SCN^-) on nanocrystalline TiO_2 electrodes," *Journal of the American Chemical Society*, vol. 115, no. 14, pp. 6382–6390, 1993.

[2] Y. Chiba, A. Islam, Y. Watanabe, R. Komiya, N. Koide, and L. Y. Han, "Dye-sensitized solar cells with conversion efficiency of 11.1%," *Japanese Journal of Applied Physics*, vol. 45, no. 24–28, pp. L638–L640, 2006.

[3] M. Grätzel, "Photoelectrochemical cells," *Nature*, vol. 414, no. 6861, pp. 338–344, 2001.

[4] J. Bisquert, D. Cahen, G. Hodes, S. Ruhle, and A. Zaban, "Physical chemical principles of photovoltaic conversion with nanoparticulate, mesoporous dye-sensitized solar cells," *Journal of Physical Chemistry B*, vol. 108, no. 24, pp. 8106–8118, 2004.

[5] A. B. F. Martinson, T. W. Hamann, M. J. Pellin, and J. T. Hupp, "New architectures for dye-sensitized solar cells," *Chemistry*, vol. 14, no. 15, pp. 4458–4467, 2008.

[6] A. Hagfeld and M. Gratzel, "Light-induced redox reactions in nanocrystalline systems," *Chemical Reviews*, vol. 95, no. 1, pp. 49–68, 1995.

[7] M. Law, L. E. Greene, J. C. Johnson, R. Saykally, and P. Yang, "Nanowire dye-sensitized solar cells," *Nature Materials*, vol. 4, no. 6, pp. 455–459, 2005.

[8] E. M. Kaidashev, M. Lorenz, H. Von Wenckstern et al., "High electron mobility of epitaxial ZnO thin films on *c*-plane sapphire grown by multistep pulsed-laser deposition," *Applied Physics Letters*, vol. 82, no. 22, pp. 3901–3903, 2003.

[9] B. Tian, X. Liu, H. Yang et al., "General synthesis of ordered crystallized metal oxide nanoarrays replicated by microwave-digested mesoporous silica," *Advanced Materials*, vol. 15, no. 16, pp. 1370–1374, 2003.

[10] H. Yang, Q. Shi, B. Tian et al., "One-step nanocasting synthesis of highly ordered single crystalline indium oxide nanowire arrays from mesostructured frameworks," *Journal of the American Chemical Society*, vol. 125, no. 16, pp. 4724–4725, 2003.

[11] J. -H. Smatt, B. Spliethoff, J. B. Rosenholm, and M. Linden, "Hierachically porous nanocrystalline cobalt oxide monoliths through nanocasting," *Chemical Communications*, vol. 10, no. 19, pp. 2188–2189, 2004.

[12] J. -H. Smatt, C. Weidenthaler, J. B. Rosenholm, and M. Linden, "Hierarchically porous metal oxide monoliths prepared by the

nanocasting route," *Chemistry of Materials*, vol. 18, no. 6, pp. 1443–1450, 2006.

[13] Y. Wang, C. -M. Yang, W. Schmidt, B. Spliethoff, E. Bill, and F. Schuth, "Weakly ferromagnetic ordered mesoporous Co_3O_4 synthesized by nanocasting from vinyl-functionalized cubic *Ia3d* mesoporous silica," *Advanced Materials*, vol. 17, no. 1, pp. 53–56, 2005.

[14] C. Dickinson, W. Zhou, R. P. Hodgkins, Y. Shi, D. Zhao, and H. He, "Formation mechanism of porous single-crystal Cr_2O_3 and Co_3O_4 templated by mesoporous silica," *Chemistry of Materials*, vol. 18, no. 13, pp. 3088–3095, 2006.

[15] P. Srinivasu, S. P. Singh, A. Islam, and L. Han, "Metal-Free Counter Electrode for Efficient Dye-Sensitized Solar Cells through High Surface Area and Large Porous Carbon," *International Journal of Photoenergy*, vol. 2011, Article ID 066901.

[16] Y. Tachibana, K. Hara, K. Sayama, and H. Arakawa, "Quantitative analysis of light-harvesting efficiency and electron-transfer yield in ruthenium-dye-sensitized nanocrystalline TiO_2 solar cells," *Chemistry of Materials*, vol. 14, no. 6, pp. 2527–2535, 2002.

[17] I. M. Arabatzis, T. Stergiopoulos, M. C. Bernard, D. Labou, S. G. Neophytides, and P. Falaras, "Silver-modified titanium dioxide thin films for efficient photodegradation of methyl orange," *Applied Catalysis B*, vol. 42, no. 2, pp. 187–201, 2003.

[18] R. E. Mistler, "Tape casting-the basic process for meeting the needs of the electronics industry," *American Ceramic Society Bulletin*, vol. 69, no. 6, pp. 1022–1026, 1990.